frontiers | Frontiers in Earth Science

TYPE Original Research
PUBLISHED 24 July 2024
DOI 10.3389/feart.2024.1401426

Check for updates

OPEN ACCESS

EDITED BY
Irene Cornacchia,
Italian National Research Council, Italy

REVIEWED BY
Eun Young Lee,
University of Vienna, Austria
Yumao Pang,
Shandong University of Science and Technology, China

*CORRESPONDENCE
Mingyou Feng,
fmyswpu@163.com

RECEIVED 15 March 2024
ACCEPTED 09 July 2024
PUBLISHED 24 July 2024

CITATION
Xia M, Zhang B, Jia S, Zhao C, Feng M, Shang J, Zhang C, Li Y and Li Y (2024), Retrogradation of carbonate platforms on a rifted margin: the late Ediacaran record of the northwestern Yangtze Craton (SW China). *Front. Earth Sci.* 12:1401426.
doi: 10.3389/feart.2024.1401426

Retrogradation of carbonate platforms on a rifted margin: the late Ediacaran record of the northwestern Yangtze Craton (SW China)

Maolong Xia[1], Benjian Zhang[1], Song Jia[1], Chunni Zhao[1], Mingyou Feng[2]*, Junxin Shang[2], Chao Zhang[2], Yong Li[1] and Yiwen Li[1]

[1]Research Institute of Exploration and Development, PetroChina Southwest Oil and Gas field Company, Chengdu, China, [2]School of Geoscience and Technology, Southwest Petroleum University, Chengdu, China

The Late Ediacaran Dengying Formation, located in the Sichuan Basin of the northwestern Yangtze Craton, is of significant interest in oil and gas exploration due to its abundant pores and vugs within microbial mound-shoal complexes. However, there is still uncertainty regarding the spatiotemporal distribution and controlling factors of the platform margin. This study comprehensively analyzes the retrogradation pattern of the Dengying Formation platform margin using seismic data, well logs, field outcrops, and petrological characteristics. Our findings reveal that the Dengying Formation strata surrounding the rift basin at the northwestern of the Yangtze Craton can be divided into three main depositional facies: basin facies, slope facies, and platform margin facies. Additionally, based on the integration of lithological, log, and seismic characteristics, the Dengying Formation is subdivided into four third-order sequences, with five sequence boundaries and three seismic facies identified. Supported by sequence stratigraphy and geophysical data, we have reconstructed the tectono-sedimentary evolution of the multiple platform margins on the eastern side of the Deyang-Anyue rift in the Sichuan Basin during the late Ediacaran. Our findings indicate that the platform underwent two phases of retrogradation. The second-stage platform margin underwent retrogradation towards the interior, spanning a distance between 10 and 80 km, based on the initial configuration established by the first-stage platform margin. The main controls for progradation and retrogradation of carbonate platforms are eustatic sea-level changes and tectonic activity. Eustatic sea-level changes can be divided into constructive and destructive phases. Constructive phases are commonly observed in highstand systems tracts, while destructive phases are often associated with transgressive systems tracts and are related to platform retrogradation processes. However, sea-level changes alone cannot fully control the process of platform retrogradation. The thermal subsidence following mantle plume events likely played a significant role in the retrogradation of the platform in the study area. During this period, tectonic processes controlled the geometry of the platform and the deposition of carbonates in the platform margin-slope-basin environment. Additionally, karst-related mound-shoal complexes developed extensively along the platform margin of the Dengying Formation in the northwestern Yangtze Craton. The Lower Cambrian dark shales represent high-quality hydrocarbon source rocks, while the Dengying Formation exhibits an optimal source-reservoir configuration.

KEYWORDS

late Ediacaran, Dengying Formation, mound-shoal complex, Yangtz Craton, rift basin, platform retrogradation

1 Introduction

The evolution of the carbonate platform has been intensively studied (Read, 1985; Reijmer, 1998; Burgess, 2001). Various studies have examined geological strata from the Paleozoic to the Cenozoic worldwide, including the progradation and subsequent retrogradation during the late Paleocene isolated carbonate platform in northern central Egypt (Shehata et al., 2020), platform-to-slope evolution during the late Cretaceous in the Western Desert of Egypt (Scheibner et al., 2003), and the platform-to-basin transition processes in southern Italy (Borgomano, 2000). They all accounted for the platform evolution process, considering the overall geometry of seismic sections (Adams and Schlager, 2000) and the changes in lithofacies, and established detailed sequence stratigraphic frameworks of the basin. In addition to investigating the evolution process of platforms, research on the factors controlling platform evolution is also common. Reijmer (1998) summarized the factors controlling the progradational and retrogradational patterns of carbonate platforms and suggested that the most important factor is the available accommodation space, which is dependent on basin depth, platform configuration and eustatic sea-level variations. However, sea-level changes are not always the sole cause of variations in the stacking patterns of carbonate platform deposits. Climatic factors, changes in transport rates, and productivity can also produce similar stacking patterns (Burgess, 2001). Tectonic condition is additional factor that controls the evolution of a platform margin (Read, 1985). However, there are few reports on the evolution of the Ediacaran carbonate platform in the Neoproterozoic era. The late Ediacaran Dengying Formation was formed as a marine platform and served as a significant gas reservoir in the Sichuan Basin (western Yangtze Craton, southwestern China) (Cui et al., 2019; Hu et al., 2019). Despite several decades of research on gas exploitation in the Dengying Formation (Dai, 2003), our understanding of the paleogeographic patterns in the northwestern margin of the Yangtze Craton during the late Ediacaran period remains incomplete due to multiple tectonic and sedimentary events (Li et al., 2014; Wang et al., 2014; Liu et al., 2015; Wang et al., 2017). The complex paleogeographic configuration and distribution of lithofacies have given rise to conflicting opinions on the processes of late Ediacaran platform retrogradation and hydrocarbon accumulation (Du et al., 2016; Li et al., 2022; Ma et al., 2022; Li et al., 2023). Therefore, it is crucial to obtain a comprehensive understanding of the paleogeographic configuration of the Dengying Formation, in order to accurately evaluate the potential for hydrocarbon production in the Sichuan Basin. Additionally, integrating this information into the broader sedimentological and stratigraphic framework of the region is essential.

Although Du et al. (2016) dealt with the late Ediacaran intracratonic rift in the Sichuan Basin; there is limited data available on the evolution of carbonate platform of the Dengying Formation despite its significant interest in hydrocarbon exploration. The main objectives of this study are as follows: 1) the establishment of paleogeographic configuration of the basin, with a specific focus on the late Ediacaran succession, and 2) to understand and interpret the processes of platform retrogradation. Overall, this study can provide information relevant to those working within this and adjacent basins for academic and industrial purposes as well as providing an example that can be compared globally to paleogeographic configuration within petroliferous basins.

2 Geological setting

The Yangtze Craton was part of the Rodinia supercontinent since the Jinning Orogeny (Tonian), leading to the formation of a unified basement. A series of studies have shown that mantle plume/superplume activities significantly contributed to the tectonic and magmatic events during this period (830–740 Ma) (Figure 1A) (Li, 1999; Li et al., 2003a; Li et al., 2003b). The primary evidence is the komatiite from the Yiyang region, dated to approximately 825 Ma, with source mantle potential temperatures reaching ~1618°C, suggesting it is likely a product of high-degree partial melting of an anomalously hot mantle plume (Wang et al., 2007). Simultaneously, the magmatic events also responded to the formation of the South China Neoproterozoic continental rift basins (Wang and Li, 2003), forming a series of extensional normal faults and featured graben or half-graben structural styles in the Nanhua rift basin in the central Sichuan Basin (Gu and Wang, 2014; Wei et al., 2018). After the rift basin stage, the Yangtze Craton transitioned into an overall thermal subsidence basin stage, corresponding to the late stage of the Rodinia breakup (Yang et al., 2020). During this time, a series of intracratonic rift basins formed in the Ediacaran, such as the Deyang-Anyue rift and the Chengkou-E'xi rift (Wang et al., 2020; Figures 1B, 2A).

During the Ediacaran, the Sichuan Basin experienced a phase of minor extension, with widespread syn-depositional faults which is developed during post-rift thermal subsidence stage (Zhong et al., 2013; Wei et al., 2015; Yang et al., 2020). The tectonic deformation styles are well matched with the tectonic structures of the Sichuan Basin extension phase, documented in the South Atlantic Ocean, the Gulf of Mexico, and the Songliao Basin (Dupré et al., 2007; Roure et al., 2009; Liu et al., 2022). The extension phase resulted in the development of graben or half-graben within the basin-fill successions during the Ediacaran, and may have controlled the

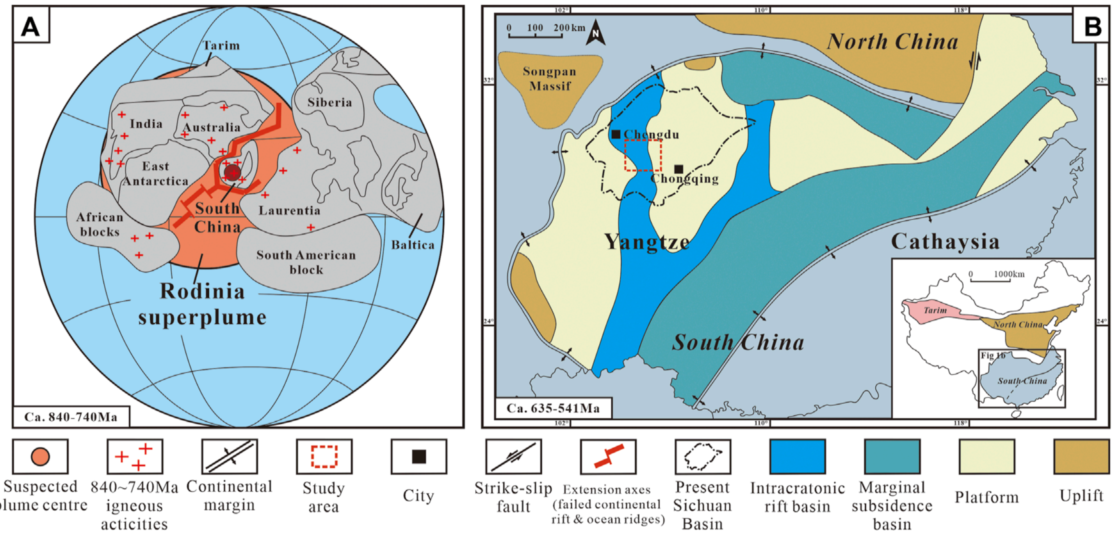

FIGURE 1
Palaeogeography position of South China, modified from Li et al. (2003b) **(A)**, and distribution of prototype basins of Yangtze Craton in the Ediacaran period, modified from Yang et al. (2020) **(B)**.

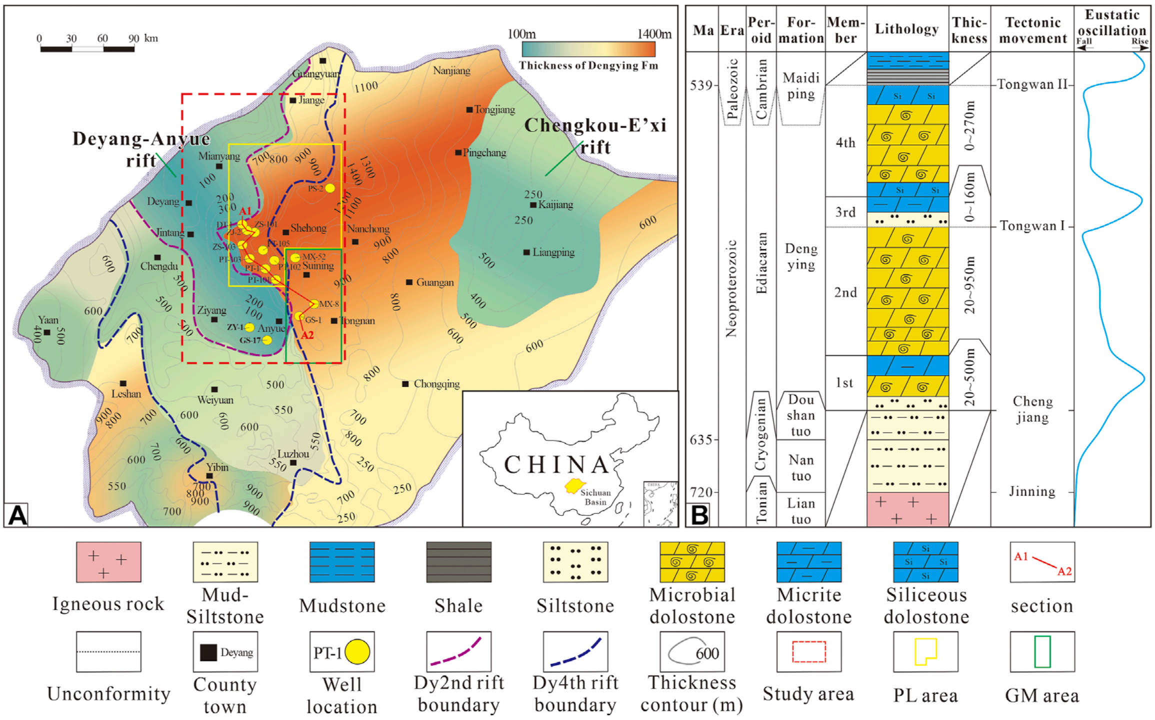

FIGURE 2
Paleo-rift distribution and thickness map of the Dengying Formation in the Sichuan Basin **(A)** and generalized Neoproterozoic to Paleozoic stratigraphy **(B)**.

dynamics of depositional systems from the platform to deep water within the rift basins during the Ediacaran.

After the Nantuo glaciation, the Yangtze Craton experienced widespread marine transgression, gradually developing into a carbonate platform (Figure 1B). The Ediacaran strata in the northwestern Yangtze Craton are primarily marine sediments, consisting of the Doushantuo and Dengying formations (Figure 2B). The Doushantuo Formation is mainly composed of shale (Wang et al., 2019). The Dengying Formation comprises a series of transgressive and highstand systems (Wang et al., 2020), which can be further divided into the Deng 1 Member, Deng 2 Member, Deng 3 Member, and Deng 4 Member. During the deposition of the Deng 1 Member, the Upper Yangtze platform experienced further transgression, causing a rise in sea level and the development of micrite dolostone and microbial dolostone. The deposition of the Deng 2 Member marked a shift in transgression to regression cycles. Subsequently, the sea level decreased, resulting in lithologies primarily comprising thrombolitic dolostone, stromatolitic dolostone, dolarenite, and powder crystal dolostone. The Deng 3 Member was characterized by a rapid transgression and significant influx of terrestrial material (Zhou et al., 2015; Deng et al., 2020), resulting in the deposition of siltstone and mudstone, interbedded with thin layers of dolostone and chert. This sedimentation exhibited distinct mixed characteristics. During the deposition of the Deng 4 Member, the sea-level declined leading to the deposition of microbial dolostone, dolarenite, and micrite dolostone with siliceous bands. The overlying Cambrian Maidiping Formation primarily consists of shale and contains siliceous shale (Figure 2B).

Drilling data indicate that the Dengying Formation in the Sichuan Basin has a thickness ranging from 100 to 1,400 m. The variation in thickness is attributed to tectono-sedimentary events, such as the Tongwan movement (Wen et al., 2021). Generally, the central and northern areas of the basin have greater thicknesses, while the western and eastern regions are thinner. The thinnest occurrence, measuring 100–200 m, is observed in the Deyang-Anyue Rift in the northwest (Figure 2A). This study focuses on the northern region of the central Sichuan Basin, specifically the area east of the Deyang-Anyue Rift, which includes the Penglai (PL) and Gaomo (GM) gas fields (Figure 2A). In this study area, tectonic differentiation is observed (Wang et al., 2017), and the platform margin of the Dengying Formation is characterized by the extensive development of microbial mounds and shoals. This feature is significant for oil and gas exploration and development.

3 Material and methods

The primary datasets utilized in this study include three-dimensional (3D) seismic data, well data, field observations, sampling, and detailed facies mapping. These were acquired from the Penglai gas fields, supplemented by outcrop observations and laboratory studies. The 3D seismic data (post-stack depth migration data) were acquired with a 4-millisecond sampling interval and a bin size spacing of 25 m (in-line) by 12.5 m (cross-line).

These seismic profiles were extracted from (3D) survey in both sides of intracratonic rift basin in the Sichuan Basin. Moreover, well log-data of resistivity logs, gamma ray logs, sonic logs, and porosity logs were also examined to confirm the interpretation that was obtained by the seismic profiles. The well-logging data were interpreted from four deep wells dug in the basin (Figures 4, 5A).

Throughout this study, lithologies and sequence boundaries of the studied succession were defined according to the description of cuttings that were extracted and analyzed from the mud logs, and also from the interpretations of the other log datasets (gamma ray, porosity, density and resistivity logs) coupled with the synthetic seismic records (Figure 5). The seismic sections were used to subdivide the Ediacaran successions into its components of seismic facies, based on their characters, type of truncation, boundaries, and stacking pattern.

Four field outcrops and 186 m cores from seven wells were meticulously observed and sampled for petrography and sedimentary facies. The sedimentary lithofacies were characterized through outcrop observations, while the laboratory study, focusing on microscopic observations, was performed at Southwest Petroleum University. 235 samples and 596 thin sections have been studied under an optical microscope (Olympus BX53M) for the microfacies and reservoir characterization. In particular, grain types and sizes, textures, diagenetic features, and reservoir space types have been reported.

4 Results

4.1 Sedimentary facies associations

The following two Ediacaran facies belts can be distinguished: (1) platform margin, and (2) slope to basin. They reflect an overall paleobathymetric trend from the platform in the east to the basin in the west and are composed of two facies associations. These facies associations comprise different subfacies types with a genetic relationship. In this study we focus on the evolution of platform margin and refrain from listing all individual subfacies types. So, platform margin can be further divided into mound-shoal complexes and intermound (or intershoal) depressions.

4.1.1 Platform margin facies

The platform margin extends along the slope-break zone between the Dengying Formation carbonate platform and the Deyang-Anyue Rift, mainly distributed on the eastern side of the rift near the open sea, influenced by wave activity. This area exhibits high-energy depositional environments and abundant microbial proliferation. The primary development includes large-scale mound-shoal complexes and intershoal depressions. The mound-shoal complexes are characterized by widespread microbial dolostone, often composed of microbial mound and grain shoal deposits, primarily developing stromatolitic dolostone (Figure 3A), thrombolitic dolostone (Figure 3B), and arenaceous dolostone (Figure 3C). Influenced by the Tongwan movement, the tops of the mound-shoal complexes in the second and fourth members of the Dengying Formation experienced epigenetic karstification (Yang et al., 2021), resulting in numerous non-selective dissolution such as solution pores and vugs (Figure 3D), forming porous reservoir. Intershoal depressions are typically located between mound-shoal complexes, with sediment deposition towards the center of these low-lying areas, forming dense reservoir in semi-deepwater environments. The lithology of these dense zones is fenestral mud-fine crystalline dolostone, but the fenestral pores are completely filled with dolostone cement (Figures 3E, F).

4.1.2 Slope to basin facies

Although there are no exploratory wells encountering slope-basin facies in the study area, outcrop and previous research suggest the development of slope-basin facies deposits in the Deyang-Anyue Rift. (1) The Lin'ansi (LAS) to Jinfeng (JF) profile in northern Sichuan shows that the Ediacaran strata comprise

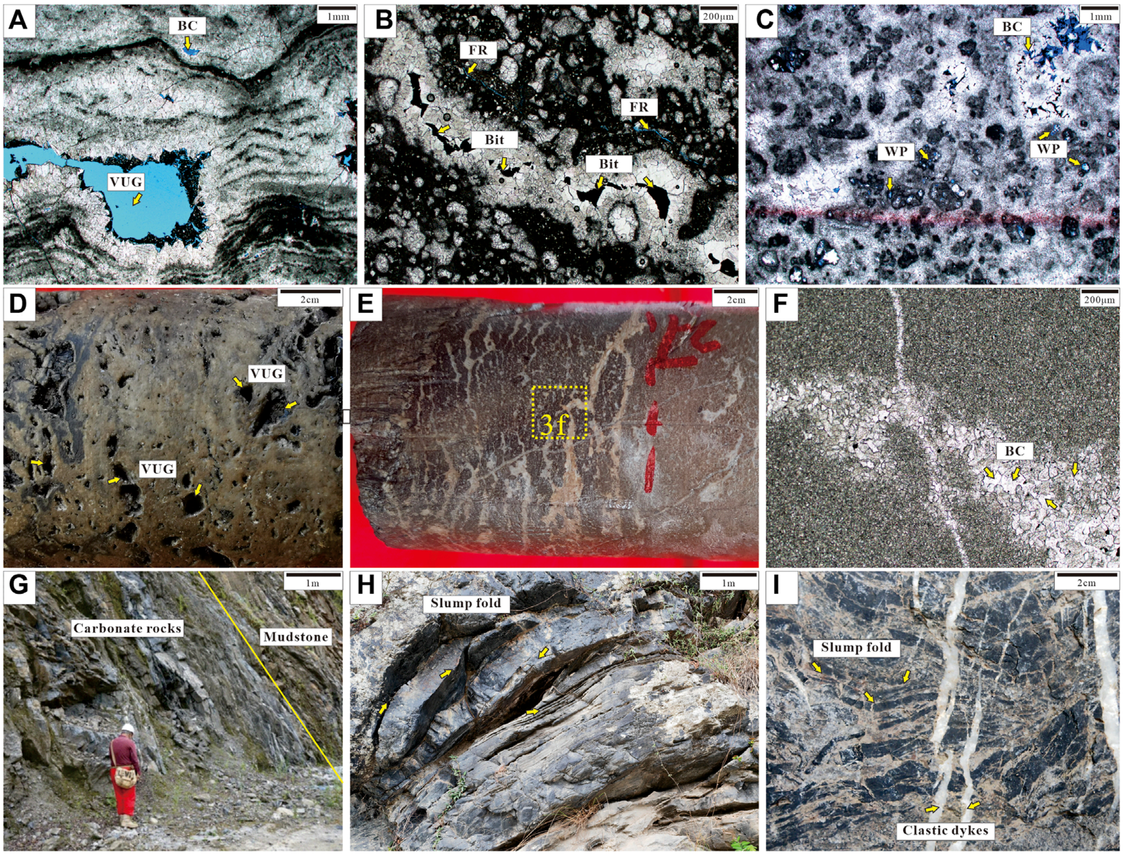

FIGURE 3
Petrographic observations of the Dengying Formation **(A)** stromatolitic dolostones, elongated vug and intercrystal pores (BC, blue) along laminae, cast thin section (doubly polished thin section impregnated with blue epoxy), at depth of 7756.25 m of well PS-2; **(B)** Thrombolitic dolostone, note that channel and vug porosity is cemented by dolostone and bitumen (Bit), cast thin section, at depth of 5845.56 m of well PT-105. **(C)** Sandy dolostone, intercrystal (BC) and intraparticle porosity (WP) are developed, cast thin sections, at depth of 7784.20 m of well PS-2. **(D)** Solution vugs (yellow arrow) along thrombolite-framework pores in thrombolite-framework dolostone, at depth of 7801.52 m of well PS-2. **(E)** Fenestral porosity in a micrite dolostone have been cemented by dolostone, at depth of 5942.77 m of well PT-105. **(F)** Micrite dolostone, intercrystal porosity (BC) are observed. **(E)** microscopic features (yellow box), at depth of 5942.77 m of well PT-105. **(G)** Mudstones was deposited over the Dengying Formation, Jinfeng (JF) section. **(H)** Slope of the Dengying Formation is dominated by slump fold, Lin'ansi (LAS) section. **(I)** Clastic dykes cross-cutting different slump bodies and their undeformed layers, mostly vertical or oblique to the bedding, host rock may be seen in lower layer, LAS section.

slope-basin facies, including black mudstone, chert, and slump deformation structures (Figures 3G–I); (2) Drilling at Well Gaoshi-17 and Well Ziyang-1 reveals that the Dengying Formation contains abundant nodular micritic dolostone, argillaceous dolostone, and siliceous mudstone, indicative of deep-water slope-basin facies (Zhou et al., 2017); (3) The Dengying Formation thins from the platform towards the rift, with seismic facies transitioning from mound-like, chaotic, and discontinuous weak reflections on the platform to sheet-like, parallel, and continuous strong reflections within the rift (Zeng et al., 2017).

4.2 Sequence stratigraphy

4.2.1 Sequence stratigraphic framework

Previous studies focusing on the Yangtze Craton have suggested that the Ediacaran Dengying Formation can be divided into four third-order sequences (Mei et al., 2006; Figure 4A). Specifically, the first and second members correspond to two third-order sequences (SQ1, SQ2), and the third and fourth members correspond to two third-order sequences (SQ3, SQ4). This study, based on existing well logging data (Liu et al., 2021; Peng et al., 2021; Tan et al., 2022), provides a comprehensive interpretation of the Dengying Formation. Five third-order sequence boundaries were identified: the base of the first member (SB1) (Figure 4B), the boundary between the first and second members (SB2) (Figure 4C), the boundary between the second and third members (SB3) (Figure 4D), the boundary between the third and fourth members (SB4) (Figure 4D), and the boundary between the fourth member and the Cambrian (SB5) (Figure 4D). Accordingly, the Dengying Formation is divided into four third-order sequences, from bottom to top: SQ1, SQ2, SQ3, and SQ4. Each sequence consists of a transgressive systems tract and a highstand systems tract.

4.2.2 Recognition of sequence boundaries

SB1 is the sequence boundary between the Dengying Formation and the Doushantuo Formation. Well data (Figure 4B) indicate

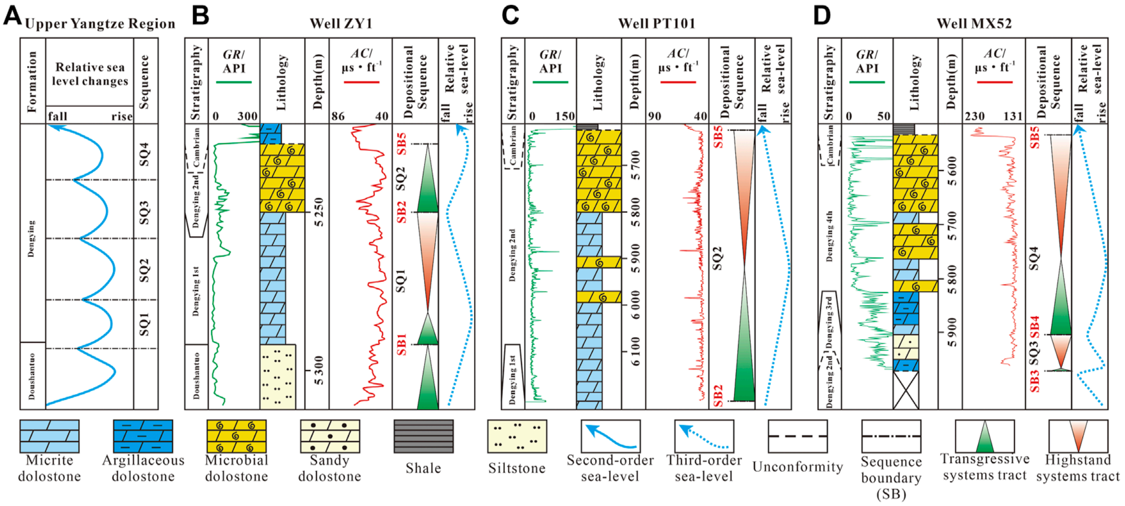

FIGURE 4
Stratigraphic division of the Dengying Formation in the upper Yangtze region, modified from Mei et al. (2006) **(A)** and Sichuan Basin, and sequence boundary recognition, modified from Tan et al. (2022) **(B–D)**.

that well ZY1 in the rift encountered light brownish-gray fine crystalline dolostone in the Dengying Formation. Below the dolostone, sandstone and mudstone deposits were identified, with the gamma and acoustic difference curves generally exhibiting high values. These characteristics suggest that these strata belong to the Doushantuo Formation (Liu et al., 2021). SB2 is the sequence boundary between the first and second members of the Dengying Formation (Figure 4C). Above this boundary, the second member is composed of shallow-water carbonate platform deposits, primarily light gray microbial dolostone and grain dolostone. The gamma curve transitions from a sawtooth pattern with high values below SB2 to a boxcar pattern with low values above it. SB3 is an unconformity formed by the first episode of the Tongwan movement, marking the sequence boundary between the second and third members of the Dengying Formation (Figure 4D). The depositional characteristics of the third member vary across different regions of the Upper Yangtze Craton but are characterized by mixed platform deposits in the study area, including black shale and argillaceous dolostone. The gamma curve transitions from a boxcar pattern with low values below SB3 to a sawtooth pattern with high peak values above it. SB4 is the sequence boundary between the third and fourth members of the Dengying Formation (Figure 4D) and represents a lithofacies transition surface. This boundary marks the transition from arenaceous dolostone to micritic dolostone. The fourth member is characterized by shallow-water carbonate platform deposits, primarily microbial dolostone. The top of this member shows epigenetic karst breccias and other karst features. At SB4, the gamma curve shows a relative increase, transitioning to a moderately sawtooth pattern with high values upward (Tan et al., 2022). SB5 is an unconformity formed by the second episode of the Tongwan movement. Due to varying degrees of erosion in the Upper Yangtze region, the strata below this boundary may consist of the second, third, or fourth members of the Dengying Formation. Above SB5 are deep-water Cambrian deposits, primarily carbonaceous mudstone and shale, with the gamma curve transitioning from a moderately sawtooth pattern with low values to high peak values (Figure 4D).

4.3 Seismic facies and distribution of platform margins

4.3.1 Seismic facies feature of platform margins

Different depositional facies exhibit distinct seismic characteristics, often reflected in variations in reflection structure, amplitude, and velocity on seismic profiles (Sheriff, 2012). By integrating geological, drilling, and seismic data, the analysis of well-tied seismic profiles (Figure 5A) identified three main seismic facies in the study area: mound-shaped seismic facies (I), clinoform seismic facies (II), and sheet-like seismic facies (III). It is believed that facies I and II represent favorable reservoir seismic facies, while facies III represent dense seismic facies.

Mound-shaped seismic facies (I) are characterized by weak-to-strong variable amplitude wavy reflections at the top, with weak-to-moderate chaotic or worm-like internal reflections (Figures 5B–D). These facies correspond to microbial mounds within the mound-shoal complexes in the study area, primarily forming in areas of higher paleotopography. Karst-type reservoirs can develop under atmospheric freshwater dissolution.

Clinoform seismic facies (II) typically exhibit moderate-to-strong variable amplitude reflections, often accompanied by wavy reflections. Occasionally, they appear as spotted weak variable amplitude reflections, with some areas showing S-shaped oblique progradation (Figure 5D). These facies represent grainstone deposits within the mound-shoal complexes, forming in high-energy, turbulent water environments. Continuous agitation by the water results in the progradational depositional pattern characteristic of these seismic reflections.

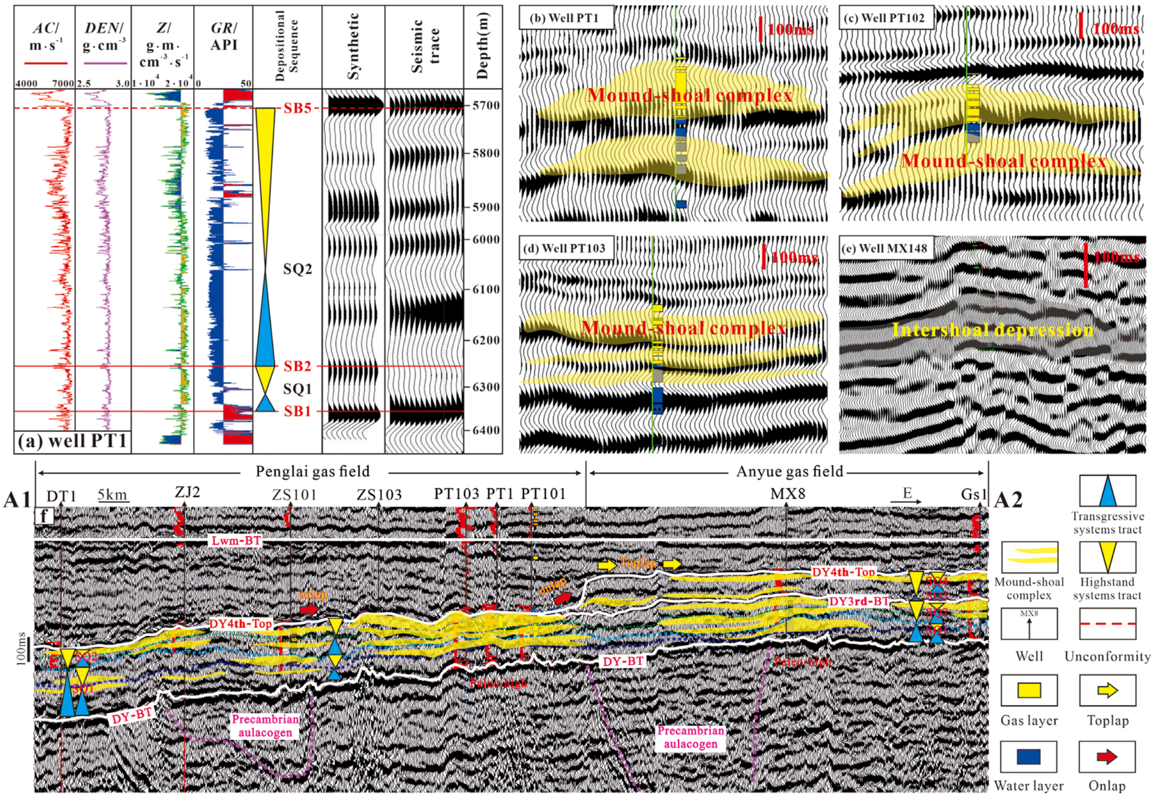

FIGURE 5
Synthetic seismogram **(A)**, typical seismic facies **(B–E)** and seismic profile of platform margin **(F)**. Line A1–A2 is shown in Figure 2A. The horizon of the bottom (BT) of the middle Cambrian longwangmiao formation (Lwm) was flattened, the Lower Cambrian strata show onlap or toplap against the platform margin of the Dengying Formation.

Sheet-like seismic facies (III) display strong single-axis reflections or blank reflections, with upper and lower boundaries that are parallel or sub-parallel to the internal reflections (Figure 5E). These facies correspond to inter-mound or inter-shoal depression deposits, forming in low-energy environments with lower paleotopography. They are often associated with higher amounts of micritic or argillaceous dolostone.

4.3.2 Distribution of platform margins

Seismic and drill data reveal that the Dengying Formation of the Deyang-Anyue aulacogen underwent two distinct stages of platform margin development (Figure 5F). During the initial stage, the platform margin was primarily observed in the Deng 2 Member, while in the subsequent stage, it was predominantly distributed in the Deng 4 Member. In the southern Gaomo (GM) area, the first-stage platform margin extends laterally for approximately 15–20 km, but its range increases to 40–130 km towards the northern Penglai (PL) area. The eastern boundary of the first-stage platform margin extends to the Jiange and Penglai regions. However, due to the influence of the Tongwan movement (Wang et al., 2014), a significant portion of the Dengying Formation is absent in the first-stage platform margin. The eroded thickness of the Dengying varies from 450 to 500 m in the Gaomo area to 650–1,000 m in the Penglai area. Furthermore, the Chengdu-Leshan and Shehong-Guangyuan areas exhibit scattered occurrences of microbial mound shoals (Figure 6). By contrast, the second-stage platform margin is approximately 10–15 km in width in the Gaomo area and 20–70 km in the transitional zone towards the Penglai area. The eastern boundary of the second-stage platform margin extends to the Guangyuan-Shehong regions. The development of microbial mounds and shoals in the second-stage platform margin is more condensed compared to the first stage, with a predominance of their distribution occurring in strips on the eastern and western sides of the Nanchong-Suining area. The thickness of the platform margin in the second stage ranges from 260 to 300 m in the Gaomo area to 350–450 m in the Penglai area (Figure 7). The second-stage platform margin on the eastern side of the aulacogen are characterized by abrupt thickness changes. This characteristic is particularly noticeable in the area north of the aulacogen, where a typical second-order step-like platform margin has formed (Figure 7). In the context of multiple rapid sea level fluctuations, the Dengying Formation on the eastern side of the Deyang-Anyue aulacogen has developed a multi-stage platform margin, featuring a distinct differentiation between platform and trough, and has a thickness range from 650 to 1,000 m. The extensive presence of microbial mounds and shoals in the margin zone serves as the basis for the formation of high-quality reservoirs.

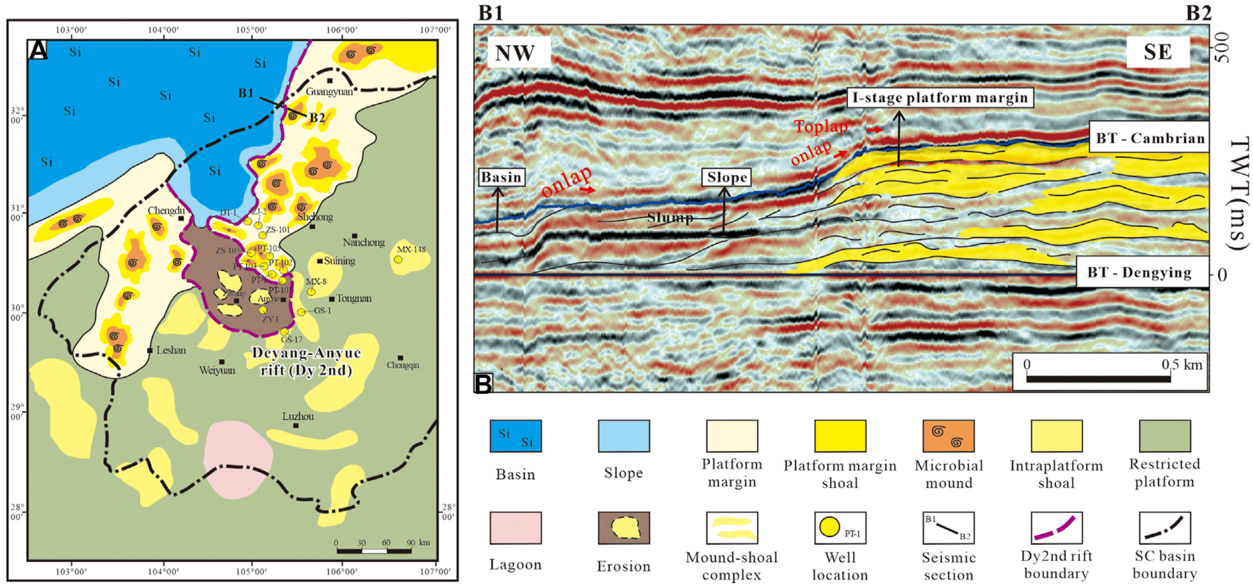

FIGURE 6
Lithofacies paleogeographic map of the Dengying 2nd (Dy 2nd) in the Sichuan (SC) Basin **(A)** and seismic section of the rift basin and I-stage platform margin of the Dengying Formation **(B)**. Line B–B′ is shown in **(A)**. The horizon of the bottom (BT) of the Dengying Formation was flattened.

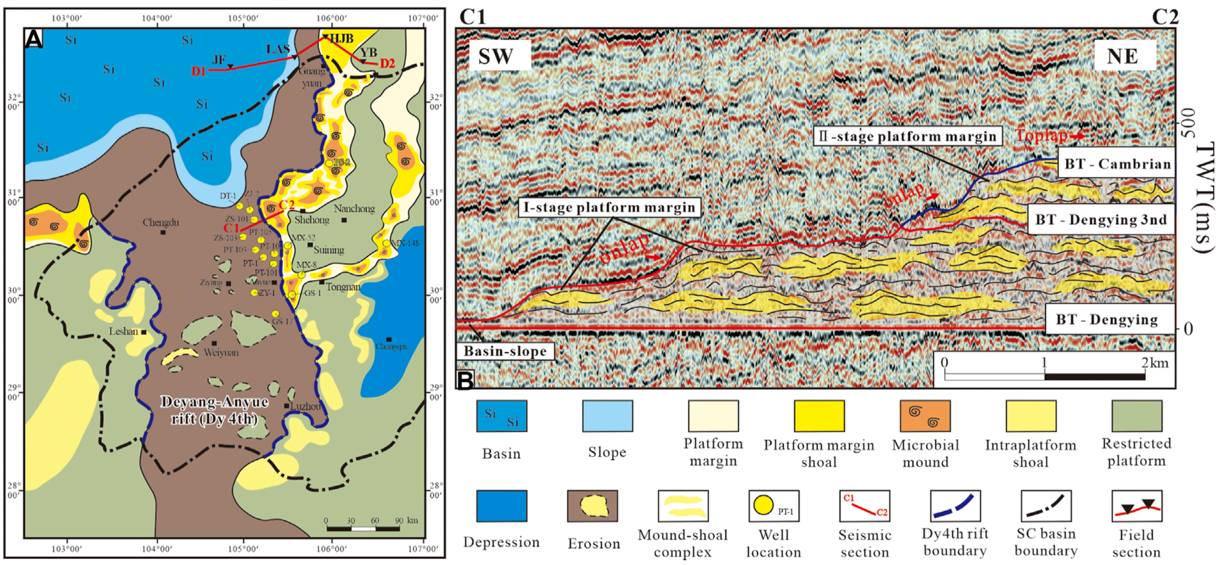

FIGURE 7
Lithofacies paleogeographic map of the Dengying 4th (Dy 4th) in the Sichuan (SC) Basin **(A)** and seismic section of the rift basin and multi-stage platform margin of the Dengying Formation **(B)**. Line C–C′ is shown in **(A)**. The horizon of the bottom (BT) of the Dengying Formation was flattened.

5 Discussion

5.1 Evolution of the carbonate platform

The features of the Deyang-Anyue rift on the northwestern margin of the Yangtze Craton have been elucidated in previous studies (Yang et al., 2014; Zou et al., 2014; Li et al., 2015; Wei et al., 2015; Xing et al., 2015; Du et al., 2016). Thus, this study emphasized the evolution process of multi-stage retrogradation of the platform margin on the eastern side of the aulacogen. The uplift and rifting of the northwestern margin of the Yangtze Craton became active during the sedimentation of the Ediacaran Doushantuo Formation and this activity can be traced back to before the deposition of the Dengying Formation. The northern margin of the Yangtze Craton experienced a significant uplift and denudation, and the rifting gradually increased after the termination of uplift (Zhu et al.,

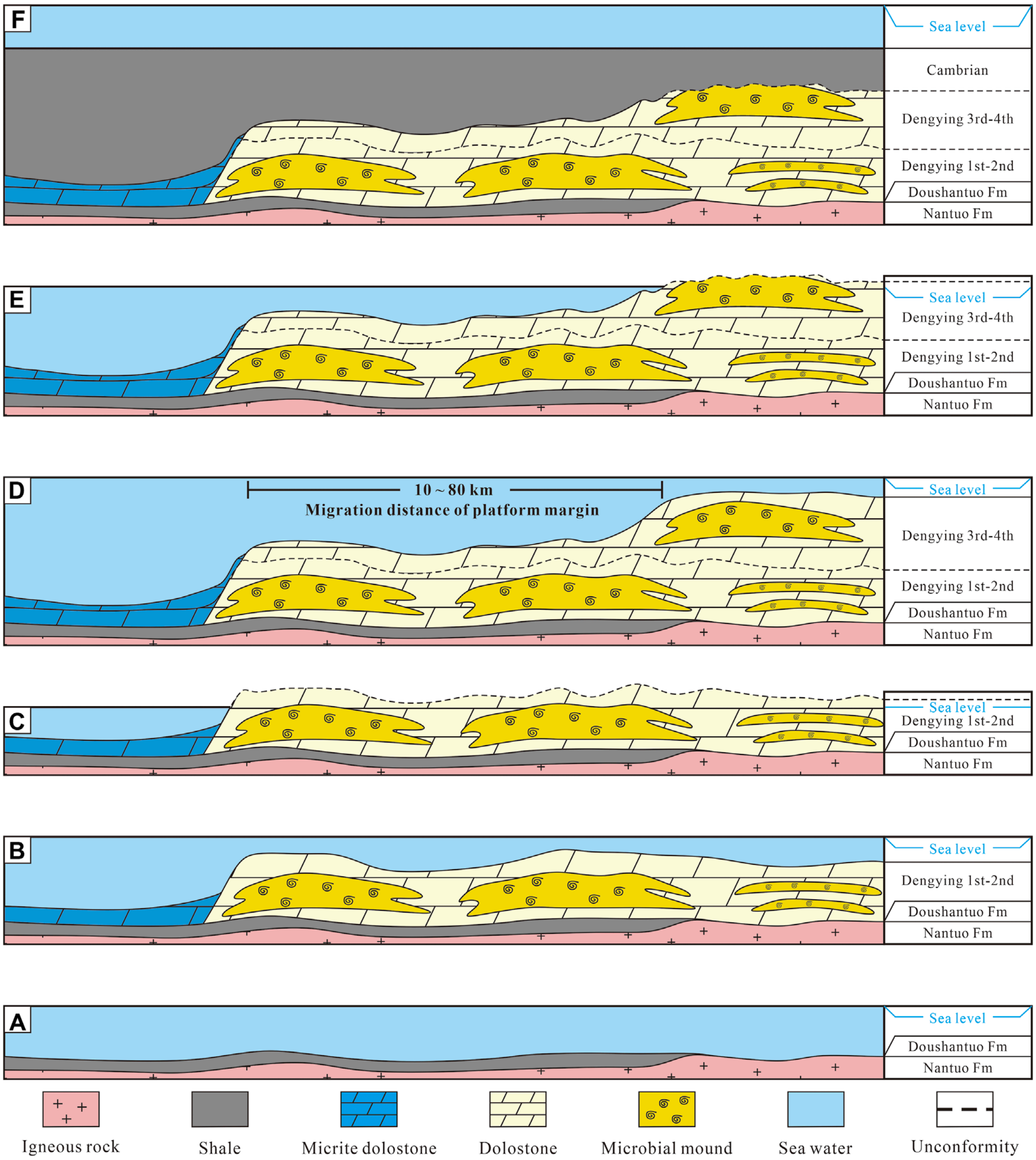

FIGURE 8
Carbonate platform margin retrogradation evolution model of the late Ediacaran in the western Yangtze Craton. **(A)** Deposition of the Doushantuo Formation. **(B)** Deposition of the Deng 1–2 Member. **(C)** Episode I of the Tongwan movement. **(D)** Deposition of the Deng 3 and 4 Members. **(E)** Episode II of the Tongwan movement. **(F)** Deposition of the Cambrian strata.

2007; Jiang et al., 2011). The Deyang-Anyue rift on the northwestern margin of the Yangtze Craton formed and started to extend southward from the Mianyang area. The sedimentary environment was predominantly characterized by basin facies. During the time, carbonate platforms had not yet formed (Figure 8A).

5.1.1 Stage A: first retrogradational phase

After deposition of the Doushantuo Formation, the carbonate platform forming initiated in SQ1 and SQ2 (deposition of the Deng 1, 2 Member). The Upper Yangtze platform experienced regional transgression, marked by a swift rapid rise in sea level and a decrease in terrigenous input while at the same time, the aulacogen extended southward to the Ziyang area. The continuous thermal subsidence (Yang et al., 2020) of the aulacogen provided conditions for the compensatory growth of the carbonate platform (accommodating space and suitable seawater environment), resulting in thick massive beds of mound-shoal complexes accumulated on the eastern side of the aulacogen (Figure 5F), while the interior of the aulacogen was dominated by slope-basin facies strata (Figure 8B). In first retrogradational phase, carbonate rock was accumulated at the edges of the original platforms. The sedimentation of carbonate rock gradually migrated into the platform with gradually decreased range, and is characterized by wedge-shaped strata on seismic profiles (Figures 6B, 7B).

After deposition of the Deng 2 Member, uplift of the strata occurred during the first episode of the Tongwan movement. The first-stage platform margin at the paleogeomorphic high experienced denudation, and an unconformity surface formed with the overlying Deng 3 Member sediments (Figure 8C). Although the rapid sea-level rise following the Nantuo glaciation (Zou et al., 2014) is considered a major factor in the first phase of platform retrogradation, we infer that the rift basin induced by thermal subsidence was the key factor in both the formation and retrogradation of the platform. However, there has been considerable debate regarding the genesis of the rift basin. Some scholars have explained the origin of the rift basin using the "eroded valley" model (Wang et al., 2014). To date, however, multiple wells drilled in the rift basin have not found glacial till or any fluvial deposits, and the east-west width of the rift basin reaches up to 300 km (Du et al., 2016). Such an erosion width is difficult to attribute solely to glacial or fluvial processes. The majority view among geologists is that extension-induced intracratonic rifting is responsible (Wei et al., 2015; Du et al., 2016; Li et al., 2018), but this does not explain the partial absence of Dengying Formation strata within the rift basin. Liu et al. (2013) proposed that the aulacogen in the late Ediacaran formed after the deposition of the Dengying Formation, and its genesis may be related to mantle plume arching, strata denudation, mantle plume collapse, and re-settlement. This hypothesis, however, directly negates the occurrence of the first episode of the Tongwan movement during the deposition of the Dengying Formation. Despite the limitations of these reports, it is important to note that tectonic activity is an unavoidable factor in the formation of the rift basin.

5.1.2 Stage B: second retrogradational phase

During the time spanning the SQ3, regional transgression resulted in the deposition of a set of strata dominated by clastic strata. The second-stage platform margin were initiated during SQ4, the aulacogen extended to the Luzhou area, and the oscillatory rising sea-level and paleogeomorphology allowed for carbonate deposition. Based on the first-stage platform edge, a retrogradation platform margin (the second-stage platform margin) was formed. Seismic data show that the lateral retrogradation distance of the second-stage platform margin, moving towards the platform interior, ranges from about 10–80 km (Figures 2, 8D). Suitable water depth and nutrient supply also provided favorable conditions for microbial propagation, which led to the development of thick mound and shoal sediments in the platform margin (Figure 8D). Following deposition of the Deng 4 Member, the second episode of the Tongwan movement caused uplift of the Deng 4 Member above to sea level, and the Deng 4 Member underwent supergene karstification (Figure 8E). Subsequently, a large area of transgression submerged the study area, and a thick layer of Cambrian mud shale was deposited on top of the Dengying Formation (Figure 8F).

In general, deposition of the Dengying Formation in the western Yangtze Craton was influenced by oscillatory sea-level rises, leading to regressive platform sedimentary sequences and the widespread development of multi-stage stepped platform margins. However, sea-level oscillation alone cannot easily change the overall characteristics of the platform. For example, the global high-frequency sea-level fluctuation during the Carboniferous-Permian ice age did not significantly impact the Late Paleozoic carbonate platforms in South China (Wang et al., 2013; Yan et al., 2015). The characteristics of carbonate platforms and their margins are also related to factors such as regional tectonic background, basement subsidence rate, biological buildup rate, and ecological accommodation space (Schlager, 1981; Schlager, 1999; Pomar, 2001; Bosence, 2005; Moore and Wade, 2013). Therefore, the study of multi-factorial constraints on the morphology of carbonate platforms should be further investigated.

5.2 Controlling factors: eustasy *versus* tectonic

The main controls for progradation and retrogradation of carbonate platforms are eustatic sea-level changes and tectonic activity (Bosellini, 1984; Everts, 1991). Retrogradation can take place only when relatively high rates of relative sea-level rise (Xia et al., 2019). In the development of the late Ediacaran carbonate platform, we may distinguish between constructive and destructive phases of relative sea-level rise. During a destructive phase, the growth or accumulation rate of carbonate rocks at the edges of the original platforms rapidly reduce or completely stop. They embody episodes of pronounced and persistent relative sea-level rise, associated retrogradation, and limitation of the areas of carbonate production (Follmi et al., 1994). Through field reconnaissance of outcrops (Figure 9A), we observed destructive phases in the transgressive systems tracts of SQ1 and SQ3. In contrast, during the constructive phase, the platform regenerated and resumed growth after a period of relative sea-level fall, leading to the extensive development of mound-shoal complexes along the platform margin. Constructive phases are observed in parasequences following marine flooding surfaces within the highstand-systems tract (Follmi et al., 1994) of SQ2 and SQ4.

However, uncertainty in the variations of sediment supply through time makes the one-to-one relationship between global eustatic changes and sequence stratigraphy very difficult to establish (Everts et al., 1995). Rapid increase in accommodation space on the platform during the late Ediacaran is not necessarily related to a rise in sea level. Reduction in carbonate growth potential during a more rapid tectonic subsidence could result in a similar stratigraphical pattern (Borgomano, 2000). The extensive Neoproterozoic bimodal magmatism in the Upper Yangtze Block and the South Qinling occurred between 850 and 720 Ma and between 720 and 600 Ma. The large-scale magmatic events are associated with the formation of the South China rift basin and breakup of the Rodinia supercontinent (Li, 1999; Ling et al., 2002). The extensive occurrence of this type of non-orogenic magmatism requires a massive and continuous heat source, which is considered to be related to the mantle superplume beneath Rodinia (Li Z. X. et al., 2003; Wang and Li, 2003; Wang et al., 2011; Zhang et al., 2016). The thermal subsidence following a sudden change in temperature at the base of the lithosphere is calculated. The calculations showed that the duration of the subsidence is on the order of 100–150 Ma (Hamdani et al., 1991), and completely cover the time required for the deposition of the Dengying Formation. Similar subsidence activities and sea-level changes also led to the

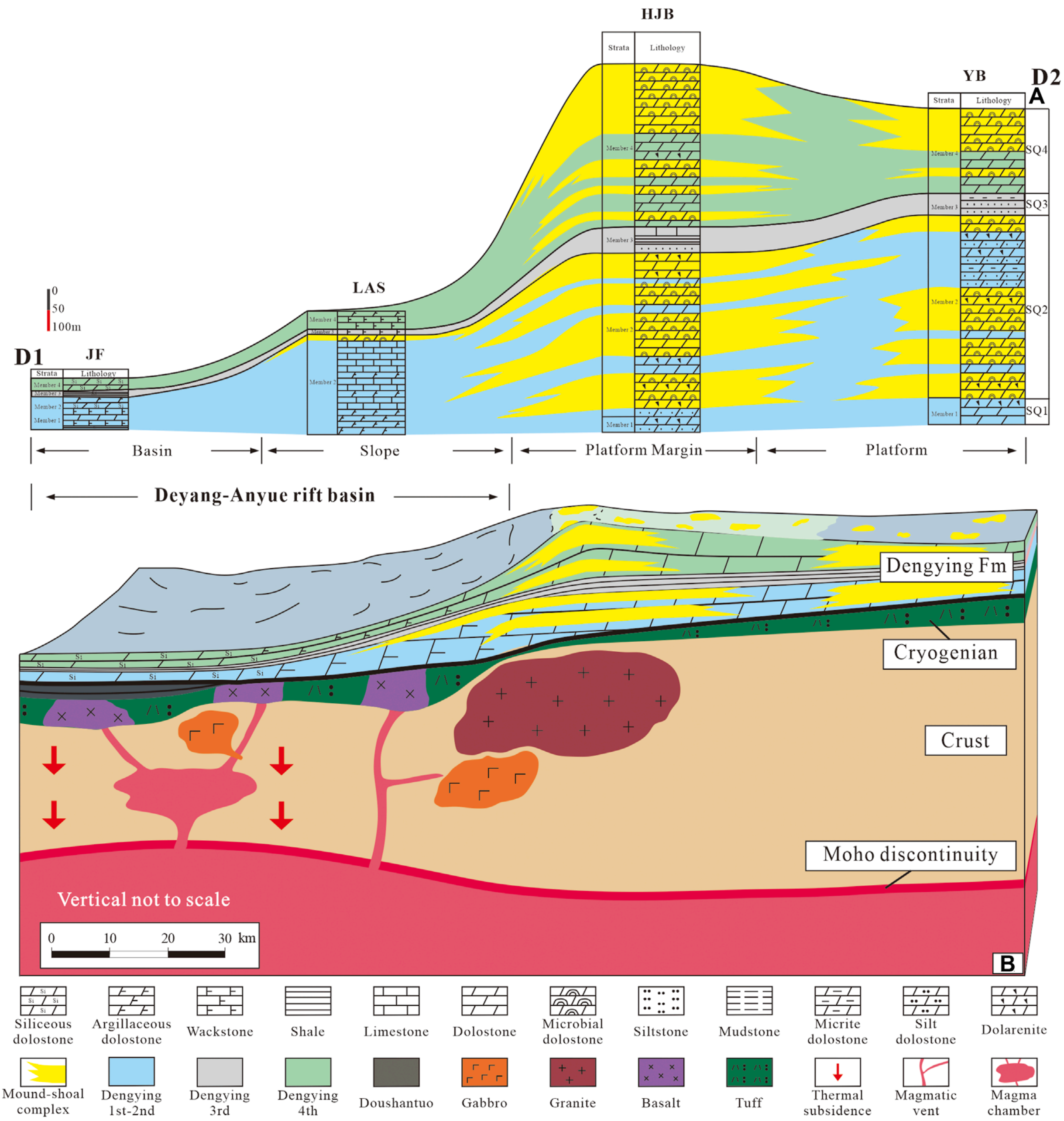

FIGURE 9
Stratigraphic illustration of measured outcrop sections in the north Sichuan Basin **(A)**, and tectono-sedimentary evolution of the platform margin to rift basin deposits in the north Sichuan Basin **(B)**. Section D1–D2 is shown in Figure 7A. The tectonic movements on the intracratonic Deyang-Anyue rift basin are hypothetical.

retrogradation of a late Paleocene isolated carbonate platform in the Galala Mountains, Eastern Desert, Egypt (Scheibner et al., 2003). Sharp et al. (2000) and Young et al. (2002) documented a similar tectonosedimentary evolution from the eastern side of the Gulf of Suez. Their three-dimensional stratigraphic structures present in the syn-rift models agree well with the largescale distribution patterns found in Scheibner et al. (2003)'s report. It is important to note that previous studies have focused on the hanging wall subsidence processes influenced by fault-related movements, providing detailed characterization of the faults. This aspect is not covered in the present study. Influenced by these paleo-tectonic events, and driven by the dynamic mechanism of thermal energy convergence within the mantle leading to uplifting, the Yangtze Craton underwent significant tectonic differentiation between the end of the Precambrian and the early Cambrian period (Wang et al., 2017), which resulted in the thinning and subsidence of the crust at the northwestern margin of the Yangtze Craton (Figure 9B), and the Deyang-Anyue rift basin developed during the late Ediacaran, forming the early paleogeomorphological of the study areas.

10.3389/feart.2024.1401426

TABLE 1 Basic characteristics and controlling factors of reservoir/source rocks of the northwestern Yangtze Craton. The data are sourced from Liu et al. (2013), Wei et al. (2013), Wang et al. (2014), Feng et al. (2017), Xia et al. (2024).

Region		Period	Strata		Sequence	Porosity	Permeability	TOC/%	Thickness	Lithology	Type	Control factors
			Formation	Member		Average/%	Average/mD		Average/m			
Central sichuan basin	Aulacogen	Cambrian	Qiongzhusi		—	—	—	0.72~2.29	>600	Organic-rich shale	Source	Tectonic subsidence
		Ediacaran	Dengying	1st~2nd	SQ1~SQ2	<1%	<0.001	—	50~200	Dolostone	Dense layer	
	II-stage platform margin	Cambrian	Qiongzhusi		—	—	—	0.07~6.57	100~400	Organic-rich shale	Source	Tectonic subsidence and sea-level oscillation
		Ediacaran	Dengying	4th	SQ4	2.02~11.69	0.006~15.80	—	0~480	Dolostone	Reservoir	
						3.84	2.36		160			
				3rd	SQ3	0.15~7.30	<0.001	0.08~7.40	0~165	Shale or argillaceous limestone	Source	
									60			
	I-stage platform margin	Ediacaran	Dengying	2nd	SQ2	2.00~11.00	0.005~10.00	—	20~270	Dolostone	Reservoir	
						4.03	1.10		110			
				1st	SQ1	<1%	<0.001	—	20~500	Dolostone	Dense layer	

As discussed earlier, the intracratonic rift basin identified on the western margin of the platform is characterized by extremely thin Dengying Formation deposits. This indicates that tectonic processes controlled the geometry of the platform and the deposition of carbonates in the slope-basin environment, even during periods of high carbonate productivity (highstand systems tract, such as SQ2 and SQ4), leading to the drowning of the Deyang-Anyue aulacogen. Therefore, we believe that late Ediacaran eustatic variations, particularly rapid sea-level rise, did not solely control the retrogradation of the platform margin in the central Sichuan area. Neoproterozoic mantle plume activity and subsequent thermal subsidence in the Upper Yangtze Craton likely controlled the geometry of the platform-to-basin transition and the retrogradation of the platform margin during the late Ediacaran.

5.3 Implication for hydrocarbon exploration

From the standpoint of a regional hydrocarbon accumulation, the highest potential reservoirs belong to the highstand system (SQ2 and SQ4) and consist of thick and widespread mound-shoal complexes of platform margin microbial dolostone sealed by Cambrian shale (Figure 8F). In contrast, the mudstone belonging to the transgressive system (SQ3) are characterized by a source potential (Wei et al., 2017). The late Ediacaran microbial dolostone units have the highest reservoir potential. These microbial dolostone is characterized by high intergranular and intragranular porosities and possible good horizontal and vertical permeabilities. Additionally, karstification has significantly enhanced the reservoir properties (Wang et al., 2014). The karst reservoirs of the shoal facies and aulacogen hydrocarbon source rocks exhibit lateral contacts between reservoirs. The monocline structural zone in the northern part of the Central Sichuan paleo-uplift is characterized by an inherited slope structure (Xie et al., 2022). The tectonic environment is relatively stable, which is conducive to lithological traps and hydrocarbon preservation. However, the formation of carbonate reservoirs is typically influenced by multi-stage tectonic events (uplift and rift) and volcanic eruptions related hydrothermal activity (Liu et al., 2019; Lee et al., 2020). Besides, depositional environment and diagenesis play a crucial rule, such as dolomitization during the syndepositional to burial stages (Feng et al., 2017; Shang et al., 2023), progressively intensified compaction with increasing burial depth (Lee et al., 2021), deep-burial hydrothermal fluid induced vugs-infillings (Feng et al., 2024). These geological processes can enhance or diminish the reservoir properties of carbonates and the hydrocarbon generation potential of source rocks.

Regarding the microbial dolostones found in the Dengying Formation in the central Sichuan Basin, data has been collected on the reservoir and source rocks in retrogradational platforms on a rifted margin. This data includes information on porosity, permeability, total organic content (TOC), thickness, and depositional sequences (Table 1). The data indicates that the microbial dolostones in SQ2 and SQ4 of the first and second platform margins during the late Ediacaran period in the central Sichuan Basin have significant characteristics such as low porosity and low permeability (Xia et al., 2024). The average porosity of SQ2 (first-stage platform) and SQ4 (second-stage platform) of the Dengying Formation in the central Sichuan Basin is 4.03% and 3.84%, respectively. Correspondingly, the average permeability measures 1.10 mD and 2.36 mD. The average thickness of the microbial dolostone reservoir is 110–160 m. In contrast, the Dengying argillaceous limestones or dolomitic limestones of SQ1 to SQ4 in the aulacogen are dense. Consequently, the organic-rich shales in SQ3 of the second platform margin, as well as the overlying Qiongzhusi Formation shales in the aulacogen, are considered to be source rocks with favorable potential for hydrocarbon generation. These source rocks possess an average TOC of 3.20% and a thickness of 370 m. Taking into account the two significant periods of weathering and erosion in the Dengying Formation of the Sichuan Basin (Wen et al., 2021), it is plausible that hydrocarbons may migrate into the reservoirs along unconformities or faults caused by tectonic activity. This presents promising opportunities for large-scale oil and gas exploration.

6 Conclusion

The late Ediacaran platform carbonates of the central Sichuan Basin are dominated by platform margin facies that transition into deeper marine carbonates through the slope. The two platform margin phases consist of mound-shoal complexes and intershoal depressions, with four third-order sequences and five sequence boundaries identified. The mound-shoal complexes are primarily developed in SQ2 and SQ4.

The retrogradation of the late Ediacaran carbonate platform margin is closely related to tectonic activity, rather than solely to eustatic sea-level changes. The deposition of the Deng 1 to 2 Formations (stage A: first retrogradational phase) was influenced by seabed paleogeomorphology induced by thermal subsidence, which controlled the initial lateral facies distribution across the first-stage platform–basin transect. The deposition of the Deng 3 to 4 Formations (stage B: second retrogradational phase) was controlled by seabed paleogeomorphology induced by both thermal subsidence and eustatic sea-level changes, leading to the retrogradation of the second-stage platform margin.

Mound-shoal complexes developed extensively in the platform margin of the Dengying Formation in the northwestern Yangtze Craton. The Lower Cambrian dark shales represent high-quality hydrocarbon source rocks, while the Dengying Formation exhibits an optimal source-reservoir configuration. Hydrocarbons can migrate along nearby unconformity surfaces and/or faults, facilitating the formation of large gas field.

Data availability statement

The raw data supporting the conclusions of this article will be made available by the authors, without undue reservation.

Author contributions

MX: Writing–original draft, Writing–review and editing. BZ: Writing–original draft, Writing–review and editing. SJ: Writing–review and editing. CuZ: Writing–review and editing. MF:

Writing–review and editing. JS: Writing–review and editing. CaZ: Writing–review and editing. YoL: Writing–review and editing. YiL: Writing–review and editing.

Funding

The author(s) declare that financial support was received for the research, authorship, and/or publication of this article. This study was supported by PetroChina Scientific Research and Technology Development (Grant No. XNS JS 2022-034 and Grant No. XNS JS 2023-032).

Acknowledgments

We would like to acknowledge the funding by PetroChina Scientific Research and Technology Development.

Conflict of interest

Authors MX, BZ, SJ, CuZ, YoL, and YiL were employed by PetroChina Southwest Oil and Gas field Company.

The remaining authors declare that the research was conducted in the absence of any commercial or financial relationships that could be construed as a potential conflict of interest.

Publisher's note

All claims expressed in this article are solely those of the authors and do not necessarily represent those of their affiliated organizations, or those of the publisher, the editors and the reviewers. Any product that may be evaluated in this article, or claim that may be made by its manufacturer, is not guaranteed or endorsed by the publisher.

References

Adams, E. W., and Schlager, W. (2000). Basic types of submarine slope curvature. *J. Sediment. Res.* 70 (4), 814–828. doi:10.1306/2DC4093A-0E47-11D7-8643000102C1865D

Borgomano, J. (2000). The Upper Cretaceous carbonates of the Gargano-Murge region, southern Italy: a model of platform-to-basin transition. *AAPG Bull.* 84 (10), 1561–1588. doi:10.1306/8626BF01-173B-11D7-8645000102C1865D

Bosellini, A. (1984). Progradation geometries of carbonate platforms: examples from the Triassic of the Dolomites, northern Italy. *Sedimentology* 31 (1), 1–24. doi:10.1111/j.1365-3091.1984.tb00720.x

Bosence, D. (2005). A genetic classification of carbonate platforms based on their basinal and tectonic settings in the Cenozoic. *Sediment. Geol.* 175 (1-4), 49–72. doi:10.1016/j.sedgeo.2004.12.030

Burgess, P. M. (2001). Modeling carbonate sequence development without relative sea-level oscillations. *Geology* 29 (12), 1127–1130. doi:10.1130/0091-7613(2001)029<1127:mcsdwr>2.0.co;2

Cui, H., Xiao, S. H., Cai, Y. P., Peek, S., Plummer, R. E., and Kaufman, A. J. (2019). Sedimentology and chemostratigraphy of the terminal ediacaran Dengying Formation at the gaojiashan section, south China. *Geol. Mag.* 156 (11), 1924–1948. doi:10.1017/S0016756819000293

Dai, J. X. (2003). Pool-forming periods and gas sources of weiyuan gasfield. *Petroleum Geol. Exp.* 25 (05), 473–480. doi:10.11781/sysydz200305473

Deng, S. L., Song, J. M., Liu, S. G., Luo, P., Li, Z. W., Yang, D., et al. (2020). Mixed sedimentary characteristics of the third member of Dengying Formation, Sichuan Basin, and its geological significance. *Acta Sedimentol. Sin.* 38 (3), 598–609. doi:10.14027/j.issn.1000-0550.2019.109

Du, J. H., Wang, Z. C., Zou, C. C., Shen, P., Zhang, B. M., Jiang, H., et al. (2016). Discovery of Intracratonicic rift in the Upper Yangtze and its coutrol effect on the formation of Anyue giant gas field. *Acta Pet. Sin.* 37 (1), 1–16. doi:10.7623/syxb201601001

Dupré, S., Bertotti, G., and Cloetingh, S. (2007). Tectonic history along the South Gabon Basin: anomalous early post-rift subsidence. *Mar. Pet. Geol.* 24 (3), 151–172. doi:10.1016/j.marpetgeo.2006.11.003

Everts, A. J. (1991). Interpreting compositional variations of calciturbidites in relation to platform-stratigraphy: an example from the Paleogene of SE Spain. *Sediment. Geol.* 71 (3-4), 231–242. doi:10.1016/0037-0738(91)90104-L

Everts, A. J., Stafleu, J., Schlager, W., Fouke, B. W., and Zwart, E. W. (1995). Stratal patterns, sediment composition, and sequence stratigraphy at the margin of the Vercors carbonate platform (Lower Cretaceous, SE France). *J. Sediment. Res.* 65 (1b), 119–131. doi:10.1306/D42681F8-2B26-11D7-8648000102C1865D

Feng, M. Y., Shang, J. X., Shen, A. J., Wen, L., Wang, X. Z., Xu, L., et al. (2024). Episodic hydrothermal alteration on Middle Permian carbonate reservoirs and its geological significance in southwestern Sichuan Basin, SW China. *Petroleum Explor. Dev.* 51 (1), 81–96. doi:10.1016/S1876-3804(24)60007-8

Feng, M. Y., Wu, P. C., Qiang, Z. T., Liu, X. H., Duan, Y., and Xia, M. L. (2017). Hydrothermal dolomite reservoir in the precambrian dengying Formation of central Sichuan Basin, southwestern China. *Mar. Petroleum Geol.* 82, 206–219. doi:10.1016/j.marpetgeo.2017.02.008

Follmi, K. B., Weissert, H., Bisping, M., and Funk, H. (1994). Phosphogenesis, carbon-isotope stratigraphy, and carbonate-platform evolution along the Lower Cretaceous northern Tethyan margin. *Geol. Soc. Am. Bull.* 106 (6), 729–746. doi:10.1130/0016-7606(1994)106<0729:PCISAC>2.3.CO;2

Gu, Z. D., and Wang, Z. C. (2014). The discovery of neoproterozoic extensional structures and its significance for gas exploration in the central sichuan Block, Sichuan Basin, south China. *Sci. China Earth Sci.* 57, 2758–2768. doi:10.1007/s11430-014-4961-x

Hamdani, Y., Mareschal, J. C., and Arkani-Hamed, J. (1991). Phase changes and thermal subsidence in intracontinental sedimentary basins. *Geophys. J. Int.* 106 (3), 657–665. doi:10.1111/j.1365-246X.1991.tb06337.x

Hu, M. Y., Gao, D., Wei, G. Q., Yang, W., and Wuren, W. (2019). Sequence stratigraphy and facies architecture of a mound-shoal-dominated dolomite reservoir in the late Ediacaran Dengying Formation, central Sichuan Basin, SW China. *Geol. J.* 54 (3), 1653–1671. doi:10.1002/gj.3261

Jiang, G. Q., Shi, X. Y., Zhang, S. H., Wang, Y., and Xiao, S. H. (2011). Stratigraphy and paleogeography of the ediacaran Doushantuo Formation (ca. 635-551 Ma) in South China. *Gondwana Res.* 19 (4), 831–849. doi:10.1016/j.gr.2011.01.006

Lee, E. Y., Kominz, M., Reuning, L., Gallagher, S. J., Takayanagi, H., Ishiwa, T., et al. (2021). Quantitative compaction trends of Miocene to Holocene carbonates off the west coast of Australia. *Aust. J. Earth Sci.* 68 (8), 1149–1161. doi:10.1080/08120099.2021.1915867

Lee, E. Y., Wolfgring, E., Tejada, M. L. G., Harry, D. L., Wainman, C. C., Chun, S. S., et al. (2020). Early Cretaceous subsidence of the Naturaliste Plateau defined by a new record of volcaniclastic-rich sequence at IODP Site U1513. *Gondwana Res.* 82, 1–11. doi:10.1016/j.gr.2019.12.007

Li, R., Wang, Y. X., Wang, Z. C., Xie, W. R., Li, W. Z., Gu, M. F., et al. (2023). Geological characteristics of the southern segment of the late sinian-early cambrian Deyang-Anyue rift trough in Sichuan Basin, SW China. *Petroleum Explor. Dev.* 50 (2), 321–333. doi:10.1016/S1876-3804(23)60390-8

Li, S. J., Gao, P., Huang, B. Y., Wang, H. J., and Wo, Y. J. (2018). Sedimentary constraints on the tectonic evolution of Mianyang-Changning trough in the Sichuan Basin. *Oil Gas. Geol.* 39 (5), 889–898. doi:10.11743/ogg20180504

Li, X. H. (1999). U-Pb zircon ages of granites from the southern margin of the Yangtze Block: timing of Neoproterozoic Jinning: Orogeny in SE China and implications for Rodinia Assembly. *Precambrian Res.* 97 (1-2), 43–57. doi:10.1016/S0301-9268(99)00020-0

Li, X. H., Li, Z. X., Ge, W. C., Zhou, H. W., Li, W. X., Liu, Y., et al. (2003a). Neoproterozoic granitoids in South China: crustal melting above a mantle plume at ca. 825 Ma? *Precambrian Res.* 122 (1-4), 45–83. doi:10.1016/S0301-9268(02)00207-3

Li, X. H., Li, Z. X., Zhou, H. N., Liu, Y., Liang, X. R., and Li, W. X. (2003b). SHRIMP U-Pb zircon age, geochemistry and Nd isotope of the Guandaoshan pluton in SW Sichuan: petrogenesis and tectonic significance. *Sci. China Ser. D Earth Sci.* 46, 73–83. doi:10.1360/03dz9029

Li, Z. Q., Liu, J., Li, Y., Hang, W. Y., Hong, H. T., Ying, D. L., et al. (2015). Formation and evolution of weiyuan-anyue extension-erosion groove in sinian system, Sichuan Basin. *Petroleum Explor. Dev.* 42 (1), 26–33. doi:10.1016/S1876-3804(15)60003-9

Li, Z. X., Li, X. H., Kinny, P. D., Wang, J., Zhang, S., and Zhou, H. (2003c). Geochronology of Neoproterozoic syn-rift magmatism in the Yangtze Craton, South China and correlations with other continents: evidence for a mantle superplume that broke up Rodinia. *Precambrian Res.* 122 (1-4), 85–109. doi:10.1016/S0301-9268(02)00208-5

Li, Z. Y., Jiang, H., Wang, Z. C., Wang, T. S., Lu, W. H., and Lu, Z. G. (2014). Control of tectonic movement on hydrocarbon accumulation in the Sinian strata, Sichuan Basin. *Nat. Gas. Ind.* 34 (3), 23–30. doi:10.3787/j.issn.1000-0976.2014.03.004

Li, Z. Z., Shi, J. H. C., Wang, J. H., and Liang, F. (2022). Characteristics of residual hill-type reservoir of Sinian Dengying Formation in Deyang-Anyue ancient rift trough,central Sichuan and its significance for oil and gas exploration. *Nat. Gas. Geosci.* 33 (8), 1263–1275. doi:10.11764/j.issn.1672-1926.2022.04.005

Ling, W. L., Cheng, J. P., Wang, X. H., and Zhou, H. W. (2002). Geochemical features of the Neoproterozoic igneous rocks from the Wudang region and their implications for the reconstruction of the Jinning tectonic evolution along the south Qinling orogenic belt. *Acta Petrol. Sin.* 18 (1), 25–36.

Liu, C. Y., Shan, X. L., Yi, J., Shi, Y. Q., and Ventura, G. (2022). Volcanism at the end of continental rifting: the Cretaceous syn-rift to post-rift transition in the Songliao Basin (NE China). *Gondwana Res.* 111, 174–188. doi:10.1016/j.gr.2022.08.005

Liu, H., Luo, S. C., Tan, X. C., Li, L., Lian, C. B., Zeng, W., et al. (2015). Restoration of paleokarst geomorphology of sinian Dengying Formation in Sichuan Basin and its significance, SW China. *Petroleum Explor. Dev.* 42 (3), 311–322. doi:10.1016/S1876-3804(15)30021-5

Liu, J. J., Liu, H. R., Li, W. H., Xie, W. R., Jiang, H., Su, W., et al. (2021). New progress in the study of aulacogen in the Sichuan Basin—a discussion on the genetic mechanism and formation time of the aulacogen. *Geol. Rev.* 67 (3), 767–786. doi:10.16509/j.georeview.2021.03.071

Liu, S. G., Sun, W., Luo, Z., Song, J. M., Zhong, Y., Tian, Y. H., et al. (2013). Xingkai taphrogenesis and petroleum exploration from upper Sinian to Cambrian strata in Sichuan Basin, China. *J. Chengdu Univ. Technol. Sci. Technol. Ed.* 40 (5), 511-520. doi:10.3969/j.issn.1671-9727.2013.05.03

Liu, Y. Q., Zhou, D. W., Jiao, X., Feng, Q., and Zhou, X. H. (2019). A preliminary study on the relationship between deep-sourced materials and hydrocarbon generation in lacustrine source rocks: an example from the Permian black rock series in Jimusar sag, Junggar Basin. *J. Palaeogeogr.* 21 (6), 983–998. doi:10.7605/gdlxb.2019.06.067

Ma, K., Wen, L., Zhang, B. J., Li, Y., Zhong, J. Y., Wang, Y. L., et al. (2022). Segmented evolution of Deyang-Anyue erosion rift trough in Sichuan Basin and its significance for oil and gas exploration, SW China. *Petroleum Explor. Dev.* 49 (2), 313–326. doi:10.1016/S1876-3804(22)60026-0

Mei, M. X., Zhou, P., Zhang, H., Chen, Y. H., and Nie, R. Z. (2006). Sequence stratigraphic framework and its palaeogeographical background for the sinian of upper Yangtze region. *J. Palaeogeogr.* 8 (2), 219–231. doi:10.3969/j.issn.1671-1505.2006.02.008

Moore, C. H., and Wade, W. J. (2013). The impact of global tectonics and biologic evolution on the carbonate system. *Dev. Sedimentology* 67, 39–48. doi:10.1016/B978-0-444-53831-4.00003-3

Peng, H. L., Ma, K., Zhang, X. H., Wen, L., Wang, Y. L., Tian, X. W., et al. (2021). Sequence stratigraphic characteristics and sedimentary evolution model of the late ediacaran in the Sichuan Basin. *Acta Sedimentol. Sin.* 39 (6), 1440–1450. doi:10.14027/j.issn.1000-0550.2021.119

Pomar, L. (2001). Ecological control of sedimentary accommodation: evolution from a carbonate ramp to rimmed shelf, Upper Miocene, Balearic Islands. *Palaeogeogr. Palaeoclimatol. Palaeoecol.* 175 (1-4), 249–272. doi:10.1016/S0031-0182(01)00375-3

Read, J. F. (1985). Carbonate platform facies models. *AAPG Bull.* 69 (1), 1–21. doi:10.1306/AD461B79-16F7-11D7-8645000102C1865D

Reijmer, J. J. G. (1998). Compositional variations during phases of progradation and retrogradation of a Triassic carbonate platform (Picco di Vallandro/Dürrenstein, Dolomites, Italy). *Geol. Rundsch.* 87 (3), 436–448. doi:10.1007/pl00009941

Roure, F., Alzaga-Ruiz, H., Callot, J. P., Ferket, H., Granjeon, D., Gonzalez-Mercado, G. E., et al. (2009). Long lasting interactions between tectonic loading, unroofing, post-rift thermal subsidence and sedimentary transfers along the western margin of the Gulf of Mexico: some insights from integrated quantitative studies. *Tectonophysics* 475 (1), 169–189. doi:10.1016/j.tecto.2009.04.012

Scheibner, C., Reijmer, J. J. G., Marzouk, A. M., Speijer, R. P., and Kuss, J. (2003). From platform to basin: the evolution of a Paleocene carbonate margin (Eastern Desert, Egypt). *Int. J. Earth Sci.* 92, 624–640. doi:10.1007/s00531-003-0330-2

Schlager, W. (1981). The paradox of drowned reefs and carbonate platforms. *Geol. Soc. Amer. Bullet.* 92 (4), 197–211.

Schlager, W. (1999). Scaling of sedimentation rates and drowning of reefs and carbonate platforms. *Geology* 27 (2), 183–186.

Shang, J. X., Feng, M. Y., Wang, X. Z., Zhang, B. J., Xu, L., Liu, X. H., et al. (2023). Alteration effects of karstification and hydrothermalism on middle Permian Qixia formation at the Wulong section, South China. *Sci. Rep.* 13 (1), 13128. doi:10.1038/s41598-023-40334-y

Sharp, I., Gawthorpe, R., Armstrong, B., and Underhill, J. R. (2000). Propagation history and passive rotation of mesoscale normal faults: implications for synrift stratigraphic development. *Basin Res.* 12 (3-4), 285–305. doi:10.1111/j.1365-2117.2000.00132.x

Shehata, A. A., El Fawal, F. M., Ito, M., Aboulmagd, M. A., and Brooks, H. L. (2020). Senonian platform-to-slope evolution in the tectonically-influenced Syrian Arc sedimentary belt: beni Suef Basin, Egypt. *J. Afr. Earth. Sci.* 170, 103934. doi:10.1016/j.jafrearsci.2020.103934

Sheriff, R. E. (2012). *Seismic stratigraphy*. New York: Springer Science and Business Media.

Tan, L., Liu, H., Chen, K., Ni, H. L., Zhou, G., Zhang, X., et al. (2022). Sequence sedimentary evolution and reservoir distribution in the third and fourth members of Sinian Dengying Formation, Gaomo area, Sichuan Basin, SW China. *Pet. Explor. Dev.* 49 (5), 1004–1018. doi:10.1016/S1876-3804(22)60328-8

Wang, J., and Li, Z. X. (2003). History of Neoproterozoic rift basins in South China: implications for Rodinia break-up. *Precambrian Res.* 122 (1), 141–158. doi:10.1016/S0301-9268(02)00209-7

Wang, X. C., Li, X. H., Li, W. X., and Li, Z. X. (2007). Ca. 825 Ma komatiitic basalts in South China: first evidence for >1500 °C mantle melts by a Rodinian mantle plume. *Geology* 35 (12), 1103–1106. doi:10.1130/G23878A.1

Wang, X. C., Li, Z. X., Li, X. H., Li, Q. L., and Zhang, Q. R. (2011). Geochemical and Hf-Nd isotope data of Nanhua rift sedimentary and volcaniclastic rocks indicate a Neoproterozoic continental flood basalt provenance. *Lithos* 127 (3-4), 427–440. doi:10.1016/j.lithos.2011.09.020

Wang, X. D., Qie, W. K., Sheng, Q. Y., Qi, Y. P., Wang, Y., Liao, Z. T., et al. (2013). Carboniferous and Lower Permian sedimentological cycles and biotic events of South China. *Geol. Soc. Lond. Spec. Publ.* 376 (1), 33–46. doi:10.1144/SP376.11

Wang, Z. C., Jiang, H., Chen, Z. Y., Liu, J. J., Ma, K., Li, W. Z., et al. (2020). Tectonic paleogeography of Late Sinian and its significances for petroleum exploration in the middle-upper Yangtze region, South China. *Petroleum Explor. Dev.* 47 (5), 946–961. doi:10.1016/S1876-3804(20)60108-2

Wang, Z. C., Jiang, H., Wang, T. S., Lu, W. H., Gu, Z. D., Xu, A. n., et al. (2014). Paleo-geomorphology formed during Tongwan tectonization in Sichuan Basin and its significance for hydrocarbon accumulation. *Petroleum Explor. Dev.* 41 (3), 338–345. doi:10.1016/S1876-3804(14)60038-0

Wang, Z. C., Liu, J. J., Jiang, H., Huang, S. P., Wang, K., Xu, Z. Y., et al. (2019). Lithofacies paleogeography and exploration significance of Sinian Doushantuo depositional stage in the middle-upper Yangtze region, Sichuan Basin, SW China. *Petroleum Explor. Dev.* 46 (1), 41–53. doi:10.1016/S1876-3804(19)30004-7

Wang, Z. C., Zhao, W. Z., Hu, S. Y., Xu, A. N., Jiang, C. Q., Jiang, H., et al. (2017). Control of tectonic differentiation on the formation of large oil and gas fields in craton basins: a case study of Sinian–Triassic of the Sichuan Basin. *Nat. Gas. Ind. B* 4 (2), 141–155. doi:10.1016/j.ngib.2017.07.019

Wei, G. Q., Shen, P., Yang, W., Zhang, J., Jiao, G. H., Xie, W. R., et al. (2013). Formation conditions and exploration prospects of Sinian large gas fields, Sichuan Basin. *Petroleum Explor. Dev.* 40 (2), 139–149. doi:10.1016/S1876-3804(13)60017-8

Wei, G. Q., Wang, Z. H., Li, J., Yang, W., and Xie, Z. Y. (2017). Characteristics of source rocks, resource potential and exploration direction of Sinian-Cambrian in Sichuan Basin, China. *J. Nat. Gas. Geosci.* 2 (5-6), 289–302. doi:10.1016/j.jnggs.2018.02.002

Wei, G. Q., Yang, W., Du, J. H., Xu, C. C., Zou, C. N., Xie, W. R., et al. (2015). Geological characteristics of the sinian-early cambrian intracratonic rift, Sichuan Basin. *Nat. Gas. Ind.* 35 (1), 24–35. doi:10.3787/j.issn.1000-0976.2015.01.003

Wei, G. Q., Yang, W., Zhang, J., Xie, W. R., Zeng, F. Y., Su, N., et al. (2018). The pre-Sinian rift in central Sichuan Basin and its control on hydrocarbon accumulation in the overlying strata. *Pet. Explor. Dev.* 45 (2), 193–203. doi:10.1016/S1876-3804(18)30023-5

Wen, L., Luo, B., Zhong, Y., Ma, K., Yan, W., Zhang, X. H., et al. (2021). Sedimentary characteristics and genetic model of trough-platform system during the Dengying period in Sichuan Basin, China. *J. Chengdu Univ. Technol. Sci. Technol. Ed.* 48 (5), 513–524,590.

Xia, B., Zhang, G. X., Yan, W., Zhang, L., Yang, Z., and Lei, Z. Y. (2019). Architecture and development of miocene carbonate platform in the beikang basin, southern south China sea. *Acta Geol. Sin.* 93, 122–123. doi:10.1111/1755-6724.14218

Xia, M. L., Zhang, B. J., Zeng, Y. Y., Jia, S., Zhao, C. N., Feng, M. Y., et al. (2024). Main controlling factors and distribution of reservoirs of the second member of Sinian Dengying Formation in Penglai gas field, central Sichuan Basin. *Lithol. Reserv.* 36 (3), 50–60. doi:10.12108/yxyqc.20240305

Xie, J. R., Zhang, Z. L., Zhong, Y., Yang, W., Li, K. Y., He, Y., et al. (2022). New understanding and potential analysis of natural gas exploration of the Dengying Member 2 in central-northern area of Sichuan Basin. *Mar. Orig. Pet. Geol.* 27 (3), 225–235.

Xing, F. C., Hou, M. C., Lin, L. B., Xu, S. L., and Hu, H. R. (2015). The records and its dynamic genesis discussion of tectonic movement during the Late Sinian and the Early Cambrian of Sichuan Basin. *Earth Sci. Front.* 22 (1), 115–125. doi:10.13745/j.esf.2015.01.010

Yan, Y. J., Yan, J. X., and Wu, S. Q. (2015). Sedimentary records of early permian major glacial sea level falls in southern guizhou province, China. *Earth Sci.* 40 (2), 372–380. doi:10.3799/dqkx.2015.029

Yang, F. L., Zhou, X. F., Peng, Y. X., Song, B. W., and Kou, X. H. (2020). Evolution of Neoproterozoic basins within the Yangtze Craton and its significance for oil and gas exploration in South China: an overview. *Precambrian Res.* 337, 105563. doi:10.1016/j.precamres.2019.105563

Yang, W., Wei, G. Q., Xie, W. R., Liu, M. C., Su, N., Jin, H., et al. (2021). Role of paleo-uplift in the scale formation of intra-platform carbonate mound-bank body reservoirs in the Sichuan Basin. *Nat. Gas. Ind. B* 8 (5), 443–454. doi:10.1016/j.ngib.2021.08.003

Yang, Y., Huang, X. P., Zhang, J., Yang, G., Song, J. R., Song, L. K., et al. (2014). Features and geologic significances of the top Sinian karst landform before the Cambrian deposition in Sichuan Basin. *Nat. Gas. Ind.* 34 (3), 38–43. doi:10.3787/j.issn.1000-0976.2014.03.006

Young, M., Gawthorpe, R., and Sharp, I. (2002). Architecture and evolution of syn-rift clastic depositional systems towards the tip of a major fault segment, Suez Rift, Egypt. *Basin Res.* 14 (1), 1–23. doi:10.1046/j.1365-2117.2002.00162.x

Zeng, F. Y., Yang, W., Sun, A., Jin, H., Xie, W. R., Ma, S. Y., et al. (2017). Seismic recognition and zonation of the platform margin facies of the Sinian Dengying Formation in central Sichuan Basin. *Oil Gas. Geol.* 38 (6), 1079–1086. doi:10.11743/ogg20170608

Zhang, R. Y., Sun, Y., Zhang, X., Ao, W. H., and Santosh, M. (2016). Neoproterozoic magmatic events in the South Qinling Belt, China: implications for amalgamation and breakup of the Rodinia supercontinent. *Gondwana Res.* 30, 6–23. doi:10.1016/j.gr.2015.06.015

Zhong, Y., Li, Y. L., and Zhang, X. B. (2013). Features of extensional structures in pre-Sinian to Cambrian strata, Sichuan Basin. *J. Chengdu Univ. Technol. (Sci. Technol. Ed.)* 40 (5), 498–510.

Zhou, H., Li, W., Zhang, B. M., Liu, J. J., Deng, S. H., Zhang, S. B., et al. (2015). Formation and evolution of upper sinian to lower cambrian intraplatformal basin in Sichuan Basin. *Acta Pet. Sin.* 36 (3), 310–323. doi:10.7623/syxb201503006

Zhou, J. G., Zhang, J. Y., Deng, H. Y., Chen, Y. N., Hao, Y., Li, W. Z., et al. (2017). Lithofacies paleogeography and sedimentary model of sinian dengying Fm in the Sichuan Basin. *Nat. Gas. Ind. B* 4 (3), 217–224. doi:10.1016/j.ngib.2017.07.023

Zhu, M. Y., Zhang, J. M., and Yang, A. H. (2007). Integrated ediacaran (Sinian) chronostratigraphy of South China. *Palaeogeogr. Palaeoclimatol. Palaeoecol.* 245 (1-2), 7–61. doi:10.1016/j.palaeo.2007.03.025

Zou, C. N., Du, J. H., Chunchun, X. U., Wang, Z. C., Zhang, B. M., Wei, G. Q., et al. (2014). Formation, distribution, resource potential, and discovery of Sinian–Cambrian giant gas field, Sichuan Basin, SW China. *Petroleum Explor. Dev.* 41 (3), 306–325. doi:10.1016/S1876-3804(14)60036-7